Research Square

Preprints are preliminary reports that have not undergone peer review.
They should not be considered conclusive, used to inform clinical practice,
or referenced by the media as validated information.

Development of a pancreatic islet organoid platform for high- throughput drug screening for type 2 diabetes treatments

Kyoung Jin Choi
Korea Research Institute of Chemical Technology
Yoon-Ju Na
Corestemchemon
Jeong Hui Im
Korea Research Institute of Chemical Technology
Hee Min Yoo
Korea Research Institute or Standards and Science
Won Hoon Jung
Korea Research Institute of Chemical Technology
Sung Bum Park
Korea Research Institute of Chemical Technology
Byumseok Koh
Korea Research Institute of Chemical Technology
Mi-Young Son
Korea Research Institute of Bioscience and Biotechnology
Ki Young Kim
kykim@krict.re.kr

Korea Research Institute of Chemical Technology

Research Article

Keywords: Pancreatic islet organoid, Type 2 diabetes, Drug screening, Disease modeling

Posted Date: May 4th, 2026

DOI: https://doi.org/10.21203/rs.3.rs-8945994/v1

License: This work is licensed under a Creative Commons Attribution 4.0 International License.
Read Full License

Additional Declarations: No competing interests reported.

Abstract

Type 2 diabetes (T2D) is a multifactorial metabolic disease characterized by impaired glucose homeostasis and progressive β-cell dysfunction, highlighting the need for human-relevant, animal-free platforms for antidiabetic drug discovery. In this study, we report the development of an advanced three-dimensional culture–based pancreatic islet model designed to overcome the limitations of conventional two-dimensional cultures and animal models. A Human stem cell-derived pancreatic islet organoid system was established that enables the rapid and reproducible induction of T2D-associated β-cell dysfunction through the application of combined metabolic and inflammatory stressors. Importantly, the model maintains high scalability and uniformity in a 96-well format, making it suitable for high-throughput drug screening. The disease-induced islet organoids recapitulate key pathological hallmarks of T2D, including impaired glucose-stimulated insulin secretion, β-cell loss and inflammatory stress. Furthermore, validation with reference antidiabetic compounds demonstrated the platform's capability to evaluate therapeutic efficacy. Collectively, this pancreatic islet organoid-based T2D model provides a physiologically relevant and efficient tool for early-stage screening and preclinical evaluation of therapeutics targeting T2D.

1. Introduction

Type 2 diabetes (T2D) is no longer viewed merely as a systemic metabolic disorder characterized by insulin resistance; rather, it is fundamentally driven by the progressive dysfunction and loss of pancreatic β-cell identity [1]. During the early stages of disease, β-cells compensate for peripheral insulin resistance by increasing insulin secretion; however, sustained metabolic overload and chronic inflammatory stress ultimately lead to β-cell failure and a reduction in functional β-cell mass [2]. Accumulating evidence now recognizes β-cell dysfunction as a primary determinant of disease onset and progression, positioning β-cells as a central therapeutic targets in T2D [3]. Despite this clear pathophysiological understanding, the development of therapeutics that effectively preserve or restore β-cell function remains challenging. A major contributing factor is the lack of experimental models that faithfully recapitulate human β-cell pathology. Conventional two-dimensional (2D) β-cell culture systems fail to maintain mature β-cell polarity, appropriate cell–cell and cell–matrix interactions, and long-term functional stability [4]. Animal models, while valuable for studying systemic metabolic regulation and inflammation, do not adequately capture human-specific β-cell stress responses, inflammatory sensitivity, or disease trajectories due to fundamental interspecies differences. These limitations have contributed to the high attrition rate of candidate therapeutics during clinical translation [5].

Human pluripotent stem cell (hPSC)–derived islet organoids have emerged as a powerful alternative, representing one of the most advanced human β-cell models currently available. hPSC-derived β-cells provide a renewable and genetically defined human cell source, eliminating donor dependency and enabling reproducible experimentation [6]. When organized into three-dimensional, islet-like organoids, these cells experience a structurally and functionally relevant microenvironment that supports endocrine identity, stimulus-dependent insulin secretion, and enhanced long-term survival compared with 2D

cultures [7]. Accordingly, hPSC-derived islet organoids constitute a physiologically relevant platform for directly interrogating human β-cell dysfunction and therapeutic responses.

Importantly, T2D is increasingly recognized as a multifactorial stress-associated disease, in which β-cells are simultaneously exposed to chronic metabolic stress and persistent inflammatory signals. Prolonged exposure to elevated glucose and fatty acids induces endoplasmic reticulum stress, oxidative stress, and mitochondrial dysfunction, while cytokine-mediated inflammatory signaling accelerates β-cell identity loss and activates cell death pathways [8, 9]. These stress axes do not operate independently but instead synergize to drive the progressive and cumulative β-cell failure observed in patients with T2D [10]. Nevertheless, many existing in vitro T2D models rely on the application of either metabolic or inflammatory stress alone, thereby capturing only isolated aspects of disease pathology. While such reductionist approaches may be suitable for studying acute stress responses, they fail to reproduce the chronic, multifactorial nature of β-cell dysfunction characteristic of T2D [11]. Consequently, integrating metabolic and inflammatory stress within a unified experimental framework is essential for achieving disease-relevant modeling of human β-cell failure [9].

From a drug discovery perspective, early-stage screening platforms must satisfy stringent practical requirements, including reproducibility, scalability, uniformity, and compatibility with multi-well formats such as 96-well plates [12]. However, significant batch-to-batch variability in stem cell differentiation has remains a barrier to the widespread adoption of organoid-based screening platforms [13]. In this study, we establish a highly reproducible and screening-compatible human islet organoid platform. By integrating stage-specific β-cell clusters with a basement membrane-inspired extracellular matrix (ECM) scaffold, we achieved uniform organoid reconstruction suitable for 96-well-based assays. This system enables the quantitative assessment of β-cell failure under a combined metabolic and inflammatory stress paradigm that reflects the pathological milieu of T2D. Our platform successfully captures hallmark features of human β-cell dysfunction under clinically relevant stress conditions. By integrating high reproducibility with physiological fidelity, this system effectively bridges the gap between human disease modeling and translational therapeutic discovery, offering a robust tool for the identification of next-generation β-cell -protective agents.

2. Materials & Methods

2.1 H1 hESCs culture

H1 human embryonic stem cells (hESCs) were purchased from WiCell Research Institute (Madison, WI, USA). The hESCs were maintained in mTeSR^{TM}1 medium, prepared by mixing the 5· supplement with mTeSR^{TM}1 basal medium (STEMCELL Technologies, Vancouver, BC, Canada), and the culture medium was replaced daily. Cells were cultured on plates coated with growth factor–reduced Matrigel (Corning® Matrigel® Growth Factor Reduced, Cat. No. 354230; Corning, NY, USA). For passaging, hESC colonies were dissociated using ReLeSR™ (STEMCELL Technologies) according to the manufacturer's instructions. Dissociated cell aggregates were diluted at a ratio of 1:50 and seeded onto Matrigel-coated

culture plates. After seeding, cells were maintained at 37°C in a humidified incubator with 5% CO_2 until the desired cell density was reached.

2.2 Differentiation of pancreatic endocrine cells from hESCs

Pancreatic endocrine progenitor cells were generated from H1 hESCs using a previously reported stepwise differentiation protocol with minor modifications [14]. Briefly, cell differentiation was carried out through seven sequential stages; stage 0, pluripotent stem cells; stage 1, definitive endoderm; stage 2, primitive gut tube; stage 3, pancreatic progenitor 1; stage 4, pancreatic progenitor 2; stage 5, pancreatic endocrine cells; and stage 6, β-cell maturation and pancreatic islet organoid generation. To initiate differentiation, H1 hESCs were dissociated using TrypLE™ Express (Gibco, NY, USA) at 0.2 mL/cm², followed by centrifugation at 300 × g for 3 min at room temperature. The resulting cell pellet was resuspended in mTeSR™1 medium supplemented with 10 μM Y-27632 (Sigma-Aldrich, St. Louis, MO, USA) and seeded onto Matrigel-coated plates (5 μg/cm²) at a density of 0.63 × 10^6 cells/cm². On the following day, the medium was replaced with stage 1 differentiation medium containing 10 μg/mL Activin A (R&D Systems, MN, USA), 1 μg/mL basic fibroblast growth factor (bFGF; R&D Systems), and 3 μM CHIR99021 (Sigma-Aldrich). Cells were incubated for 24 h at 37°C in a humidified atmosphere with 5% CO_2. Thereafter, the medium was replaced daily with stage 1 medium containing 10 μg/mL Activin A and 1 μg/mL bFGF for an additional 3 days. For induction of primitive gut tube formation (stage 2), cells were cultured in stage 2 medium supplemented with 50 μg/mL keratinocyte growth factor (KGF; PeproTech, NJ, USA) for 2 days. Subsequently, pancreatic progenitor differentiation (stage 3) was induced by culturing cells in stage 3 medium containing 50 μg/mL KGF, 2 μM TPPB (Tocris, UK), 2.5 μM Sant-1 (Sigma-Aldrich), 10 μM retinoic acid (Sigma-Aldrich), and 1 μM LDN193189 (Sigma-Aldrich) for 2 days. Cells were then further differentiated into pancreatic progenitor 2 (stage 4) by culturing for 4 days in stage 4 medium, in which the concentration of retinoic acid was reduced to 1 μM. For pancreatic endocrine differentiation (stage 5), cells were cultured for 5 days in stage 5 medium containing 2.5 μM Sant-1, 1 μM retinoic acid, 10 μM γ-secretase inhibitor XXI (Merck Millipore, MA, USA), 100 nM ALK5 inhibitor II (Enzo Life Sciences, NY, USA), and L-3,3',5-triiodothyronine (T3; Merck Millipore). Latrunculin A (1 μM; Cayman Chemical, MI, USA) was administered only during the first 24 h of stage 5. For β-cell maturation (stage 6), cells were cultured under two-dimensional (2D) conditions in stage 6 medium for 7 days. After completion of stage 6, cells were either subjected to 3D culture for pancreatic islet organoid formation or cryopreserved in CryoStor® (STEMCELL Technologies) and stored in liquid nitrogen for long-term preservation. Cryopreserved cells were thawed, stabilized on Matrigel-coated plates (10 μg/cm²) for one week in stage 6 medium, and subsequently used for 3D culture.

2.3 Generation of pancreatic islet organoid and T2D disease modeling

Cells at stage 6 were detached using Accutase™ (0.04 mL/cm^2; STEMCELL Technologies) and seeded into ultra-low attachment (ULA) 96-well plates (Corning, NY, USA) at a density of 2.5 × 10^4 cells per well

in stage 6 medium. After seeding, plates were centrifuged at 2,000 rpm for 1 min to promote uniform 3D cluster formation. To improve organoid maturation, human placenta–derived type IV collagen (hCol IV; Cat. No. 5022; Advanced BioMatrix, CA, USA) was added to the culture medium 2 days after 3D cluster formation. The resulting pancreatic islet organoids were further cultured for up to 14 days, with medium exchange performed every other day.

For induction of T2D associated β-cell dysfunction, islet organoids were exposed to a T2D induction medium containing a combination of palmitate (Sigma-Aldrich), high glucose (Sigma-Aldrich), and pro-inflammatory cytokines (R&D Systems). T2D induction was initiated 2 days after 3D cluster formation. During extended culture, either normal stage 6 medium (control) or T2D induction medium was replaced every other day.

2.4 Immunofluorescence staining

For 2D cultured cells, cells were washed twice with Dulbecco's phosphate-buffered saline (DPBS; Gibco) and fixed with 10% neutral formalin for 15 min at room temperature. Following fixation, cells were washed three times with DPBS and blocked with 5% normal donkey serum (Abcam, MA, USA) and 0.1% Triton X-100 (Sigma-Aldrich) for 1 h at room temperature. Cells were then incubated with primary antibodies diluted in blocking buffer overnight at 4°C. On the following day, cells were washed three times with DPBS and incubated with fluorophore-conjugated secondary antibodies for 1 h at room temperature in the dark. Nuclei were counterstained with DAPI (1:1000) for 5 min. Fluorescence images were then acquired using a fluorescence microscope (Nikon, Tokyo, Japan).

For 3D pancreatic islet organoids, paraffin-embedded blocks were prepared as previously described [15] with minor modifications. Briefly, 3D clusters were fixed in 10% neutral formalin for 30 min at room temperature and washed twice with DPBS (Gibco). Fixed clusters were embedded in agarose prior to paraffin processing. Specifically, samples were transferred to 1.5 mL microcentrifuge tubes and resuspended in ultra–low–gelling-temperature agarose solution (Sigma-Aldrich). Samples were centrifuged at 15,000 rpm for 30 s, excess supernatant was removed, and agarose was allowed to solidify for 5 min at − 20°C. The agarose-embedded samples were then transferred and further embedded in standard agarose to generate cell blocks.

Paraffin-embedded spheroid blocks were processed using an automatic tissue processor (Thermo Fisher Scientific, Waltham, MA, USA,) with a standard 14 h protocol and embedded in paraffin wax. Sections of 4 μm thickness were cut and mounted onto glass slides. Deparaffinization was performed by sequential incubation in 100% xylene (twice, 5 min each), followed by graded ethanol washes (100%, 90%, and 70% ethanol) and rehydration in distilled water. Antigen retrieval was carried out by incubating slides in 200 mL of pre-warmed antigen retrieval solution (Sigma-Aldrich) for 30 min, followed by rinsing under running tap water for 5 min. Immunofluorescence staining was then performed as described above for 2D cultures.

The primary antibodies used in this study included anti-FOXA2, anti-PDX1, anti-insulin, anti-chromogranin A (CHGA) (Abcam), anti-SOX17, anti-C-peptide, anti-neurogenin 3 (NGN3) (R&D Systems), anti-NKX2.2, anti-NKX6.1 (Novus Biologicals, CO, USA), anti-somatostatin (SST) (Invitrogen, MA, USA) and anti-cleaved caspase-3 (Cell Signaling Technology, MA, USA).

2.5 Lactate dehydrogenase (LDH) assay

Cell cytotoxicity was determined by measuring lactate dehydrogenase (LDH) release into the culture medium using an LDH assay kit (Promega, Madison, WI, USA). Culture supernatants were collected and immediately stored at − 80°C until analysis. LDH activity in the collected medium was measured in duplicate according to the manufacturer's instructions. In brief, culture medium was diluted into LDH storage buffer, and LDH activity was measured by adding an equal volume of LDH detection reagent to each sample.

2.6 Glucose stimulated insulin secretion (GSIS) assay

Glucose-stimulated insulin secretion (GSIS) was assessed based on a previously reported protocol with minor modifications [14]. Krebs–Ringer bicarbonate (KRB) buffer (128 mM NaCl, 5 mM KCl, 2.7 mM $CaCl_2$, 1.2 mM $MgSO_4$, 1 mM Na_2HPO_4, 1.2 mM KH_2PO_4, 5 mM $NaHCO_3$, and 10 mM HEPES; pH 7.4) supplemented with 0.1% (w/v) bovine serum albumin (BSA) was freshly prepared on the day of each experiment. Pancreatic islet organoids were washed twice with 100 µL of KRB buffer and pre-incubated in KRB buffer containing 2 mM glucose for 2 h at 37°C in a humidified atmosphere with 5% CO_2 to induce glucose starvation. After pre-incubation, the buffer was removed, and organoids were washed once with KRB buffer. Subsequently, 100 µL of KRB buffer containing either low glucose (LG; 2 mM) or high glucose (HG; 20 mM) was added to each well, and organoids were incubated for 1 h to stimulate insulin secretion. Following incubation, supernatants were collected and either immediately analyzed for insulin secretion using a human insulin ELISA kit (ALPCO, American Laboratory Products Company, NH, USA) after a threefold dilution, or stored at − 80°C until analysis.

2.7 RNA extraction and quantitative PCR analysis

Total RNA was extracted using the RNeasy Mini Kit (Qiagen, Valencia, CA, USA) according to the manufacturer's instructions. A total of 500 ng RNA was reverse-transcribed into cDNA using the AccuPower® RT PreMix kit (Bioneer, Daejeon, Korea). Gene-specific primers were designed using the NCBI Primer-BLAST tool, and the primer sequences are listed in Table 1. Quantitative real-time PCR was performed using the Rotor-Gene Q system (Qiagen). Relative gene expression levels were calculated using the comparative ΔΔCt method after normalization to the housekeeping gene 18S ribosomal RNA (18S rRNA).

For gene expression profiling, an RT² Profiler PCR Array (GeneGlobe ID: PAHS-011Z; Qiagen) was used to analyze the expression of inflammation-related cytokine genes according to the manufacturer's protocol. All qPCR reactions were performed in triplicate to ensure reproducibility.

2.8 Inflammatory cytokine secretion analysis by ELISA

The secretion levels of inflammatory cytokines were quantified using enzyme-linked immunosorbent assay (ELISA). Cell culture supernatants were collected after T2D induction, and to prevent cell carryover, only 40 µL of the total 100 µL culture medium was carefully transferred for analysis. Samples were either immediately analyzed or stored at − 80°C until use. The concentrations of C-X-C motif chemokine ligand 1 (CXCL1) and interleukin-8 (IL-8) were measured using commercially available human ELISA kits according to the manufacturers' instructions (Human CXCL1/GRO DuoSet ELISA and Human IL-8/CXCL8 Quantikine ELISA kits; R&D Systems, MN, USA). Prior to analysis, samples were diluted 5- to 10-fold as required. Absorbance was measured at 450 nm using a microplate reader (SpectraMax iD5e Multi-Mode Microplate Reader; Molecular Devices, CA, USA). Cytokine concentrations were calculated based on standard curves and expressed as pg/mL.

2.9 Flow-cytometry analysis

Islet organoids were dissociated into single-cell suspensions and subjected to intracellular staining for insulin, glucagon, and somatostatin (SST). Cells were fixed in 4% paraformaldehyde (PFA) and stored in PBS until staining. For intracellular staining, cells were washed with FACS buffer (PBS + 2% FBS) and permeabilized using 0.1% Triton X-100 in PBS containing 1% BSA. Primary/secondary antibodies were used as follows: anti-insulin (guinea pig IgG; Invitrogen, Cat# PA1-26938) detected with anti–guinea pig IgG Alexa Fluor 488 (Abcam, Cat# ab150185); Alexa Fluor 647–conjugated anti-glucagon (R&D Systems, Cat# IC1249R); and anti-somatostatin/SST (GeneTex, Cat# GTX60646, mouse IgG) detected with anti-mouse IgG Alexa Fluor 647 (Invitrogen, Cat# A-31571). Approximately 0.5 × 10^6 cells per sample were used for acquisition. Single-antibody staining controls were included for antibody titration and for establishing gating/controls. Data were acquired on a BD FACSVerse and analyzed using FlowJo v10.10.

2.10 Statistical analysis

All graphical results are expressed as means with standard deviation of the mean ± standard deviation (SD). Statistical analyses were performed using GraphPad Prism software (GraphPad Software Inc., La Jolla, CA, USA). Statistical significance was determined using multiple t-tests or a one-way ANOVA followed by Tukey's multiple comparison test. $P < 0.05$ was considered statistically significant.

3. Results

3.1 Human embryonic stem cell-derived pancreatic β-cell generation for drug screening model

Human ESC-derived pancreatic β-cell generation was based on a previously reported method [14], but was modified to establish a drug screening model that reproduces key characteristics of β-cells from patients with T2D. The overall process for model generation is illustrated in Fig. 1A. Briefly, hESCs were subsequently differentiated into pancreatic β-cells (stage 6) as described in [14], and cells were then cultured for several additional days to form spheroids using 96-well ultra-low attachment plates, followed by T2D induction and subsequent use as a screening-compatible model for evaluating drug

efficacy. Differentiation into mature β-cells was confirmed through immunofluorescence staining of stage-specific markers and by analyzing the expression of mature β-cell markers at stage 6 (Fig. 1B-D). As shown in Fig. 1B, essential stage-specific factors were appropriately expressed, and mature β-cell markers including insulin and CHGA remained expressed following cluster formation (Fig. 1C and 1D). Furthermore, Fig. 1D demonstrates that the clusters mainly consist of C-peptide$^+$/NKX6.1$^+$ β-cells, along with a smaller population of glucagon$^+$ and SST$^+$ α- and δ- cells.

The goal of this study was to establish a screening-compatible evaluation method for T2D therapeutic candidates using pancreatic β-cell clusters to create a cellular environment more closely resembling that of the human body. Because the development of a screening model composed of uniform and functionally representative tissues is essential, stage 6 immature β-cells were seeded onto 96-well ULA plates to form uniform spheroids, and a subsequent maturation protocol was required (Fig. 2A). However, during extended culture and maturation, cytotoxicity within the spheroids (Fig. 2B) and the proliferation of unclassified or undifferentiated cells (Fig. 2C, red arrows) were observed. To overcome these, collagen type IV from human placenta was added to the culture medium 2 days after cell seeding. In human pancreatic islets, extracellular matrix (ECM) molecules such as collagen type IV, VI and laminins are the key components of the basement membrane in pancreatic islets, providing structural integrity and regulating cell survival and function [16–18]. The addition of human collagen type IV (hCol IV) was during the 3D β-cell cluster formation effectively reduced organoid cytotoxicity and suppressed the growth of unclassified, non-specific cells (Fig. 2B and 2C). Furthermore, hCol IV-treated organoids showed the increase levels of C-peptide$^+$/NKX6.1$^+$ cells (Fig. 2D). In order to determine the optimal concentration of hCol IV, 5 to 20 μg/ml of hCol IV were applied for 7 and 14 days, and the insulin secretion capacity was assessed using a GSIS assay (Fig. 2E). In particular, after 14 days of extended culture, pancreatic islet organoids without hCol IV exhibited a marked reduction in insulin secretion, whereas those treated with hCol IV maintained a stable response to glucose stimulation, demonstrating the role of hCol IV in promoting β-cell maturation and functional stability. Mouse-derived laminin was also tested in the GSIS assay but had no positive effect on insulin secretion (Figure S1). From these results, a 10 μg/ml hCol IV was selected and applied to the development of a subsequent efficacy evaluation model.

3.2 Establishment of T2D model using islet organoids

In T2D, β-cell dysfunction occurs through various pathways, including inflammatory factors, glucotoxicity, and high levels of free fatty acids (FFAs) derived from a high-fat diet [19]. To induce T2D pathogenic features in pancreatic islet organoids, palmitate, high glucose, and a cytokine mixture (IL-1β and TNF-α) were applied individually or in combination for 3, 5, or 7 days, and the expression of β-cell dysfunction–related genes was analyzed by qPCR (Figure S2 and Fig. 3). During the pathogenesis of T2D, β-cells undergo dedifferentiation, cell loss and pro-inflammatory responses [20]. The expression of genes associated with β-cell dysfunction—including islet amyloid polypeptide (IAPP) production, β-cell dedifferentiation, apoptosis, inflammation, and ROS stress—was analyzed and compared (Figure S2 and

Fig. 3). Based on these results, the group treated with all three T2D induction factors was ultimately selected for further analysis. As a result, IAPP was significantly increased after 3 days of treatment, whereas the mature β-cell specific markers, insulin, PDX1, and MafB, were decreased after T2D induction. Notably, the pancreatic progenitor cell marker neurogenin 3 (ngn3) was significantly elevated in T2D induced organoids, suggesting that T2D induction involves not only a reduction in β-cell mass but also β-cell dedifferentiation [21]. Other β-cell-dysfunction-related responses including β-cell apoptosis, ER stress, inflammation, and ROS stress were also significantly increased after T2D induction.

3.3 Optimization of a drug efficacy evaluation system using a pancreatic islet organoid-derived T2D model

To optimize the drug efficacy evaluation system, several parameters, including glucose-responsible insulin secretory function and changes in cellular composition after T2D induction, were compared and analyzed (Fig. 4). First, static GSIS assay was conducted after T2D induction up to 5 days (Fig. 4A). As shown in Fig. 4A, insulin secretion began to decline compared with the control group after one day of T2D induction and showed a statistically significant decrease from day 3 (0.98-fold vs. control HG, $P < 0.01$). The reduction in insulin secretion remained significant at days 4 (0.95-fold vs. control HG, $P < 0.01$) and 5 (0.92-fold vs. control HG, $P < 0.01$). In contrast, immunofluorescence staining showed that the number of insulin-positive cells was not significantly reduced after 3 days of T2D induction. However, following 5 days of T2D induction, insulin-positive β-cells were markedly decreased, accompanied by an increase in cleaved caspase-3–positive cells (Fig. 4B). Notably, the 3-day induction condition recapitulated an early, reversible pathological state of human T2D, characterized by functional impairment without overt β-cell loss, in contrast to many in vivo models that predominantly reflect irreversible β-cell destruction. Therefore, the induction period was fixed at 3 days for subsequent experiments. The compositional changes in endocrine cell populations within the organoids following T2D induction were further investigated by flow cytometry (Fig. 4C–E). In control organoids, insulin-positive (INS^+) β-cells accounted for approximately 63.6% of the total population (Q3 gate), whereas this fraction decreased to ~ 40.7% in T2D-induced organoids. Similarly, the proportion of glucagon-positive (GCG^+) α-cells decreased from ~ 16.1% in control organoids to ~ 9.7% following T2D induction. These results indicate a moderate reduction in endocrine cell proportions without extensive cell loss, suggesting that the T2D-induced organoids recapitulate β-cell dysfunction and diabetes-associated alterations in islet cellular composition while maintaining minimal acute cytotoxicity [20–22].

Inflammation is a major pathological factor in the development and progression of T2D [22]. The expression of inflammation-related genes was analyzed; however, except for MCP-1, the gene expression levels of the pro-inflammatory cytokines IL-1β and TNFα did not show a significant increase (Fig. 3). Therefore, the effects of T2D induction on inflammatory signaling were further examined using a qPCR array approach (Fig. 4D). As a result, the expression of most inflammatory cytokine genes was upregulated following T2D induction, suggesting that inflammatory stress is also associated with β-cell dysfunction in organoids during T2D induction. Among these, CXCL1 and CXCL8 (IL-8), which exhibited

one of the most prominent increases, were further evaluated at the secretion level by ELISA (Fig. 4E). ELISA analysis showed that the secretion of CXCL1 and IL-8 was markedly increased in T2D-induced organoids, further supporting the ability of the pancreatic islet organoid model developed in this study to recapitulate inflammation-induced stress.

In addition, freezing and recovery conditions for cells at the stage 6 of 2D culture were established, enabling organoid banking for subsequent drug evaluation assays. After thawing and a brief recovery period, pancreatic islet organoids were reconstructed in 96-well plates with hCol IV, and GSIS analysis revealed that there was no significant difference in insulin secretion levels before and after cryopreservation (Fig. 4H).

3.4 Optimization of a drug efficacy evaluation system using a pancreatic islet organoid-derived T2D model

To evaluate the utility of the developed T2D model for drug testing, selected reference compounds were applied to assess the model's responsiveness, its capacity to capture reversible β-cell functional recovery, and its suitability as a preclinical screening platform (Fig. 5). The reference compounds selected for this study included exendin-4, a GLP-1 agonist; the DPP-4 inhibitor sitagliptin, and resveratrol; and the GLP-1/GIP dual agonist tirzepatide (Fig. 5). The evaluation of the experimental drugs was conducted by periodically monitoring whether GSIS was impaired in the T2D-induced organoids compared with normal organoids. Selected compounds were treated for 2 days, followed by 3 days of T2D induction. As intended, the extent to which reduced insulin secretion in the high-glucose T2D-induced organoids was restored by each treatment was comparatively assessed. As a result, reference compounds significantly increased the insulin secretion levels under T2D induction conditions, with the GLP-1/GIP dual agonist tirzepatide and the resveratrol showing the most pronounced efficacy in restoring β-cell function. To further examine differential responses between species, the effects of GSK-1292263 were additionally evaluated in human islet organoids and the rat insulinoma RIN-m5F cell line (Figure S3). In T2D-induced human islet organoids, GSK-1292263 treatment did not result in a significant change in insulin secretion (Figure S3A). By contrast, a significant increase in insulin secretion was observed in RIN-m5F cells following GSK-1292263 treatment under glucose-stimulated conditions (Figure S3B), suggesting a differential between the two experimental models.

4. Discussion

In this study, we established a screening-compatible human pancreatic islet organoid platform that enables the induction and evaluation of type 2 diabetes (T2D)-associated β-cell dysfunction. This system successfully recapitulates key pathological features of T2D and provides a reliable platform for evaluating the therapeutic efficacy of candidate compounds. In addition, by incorporating human collagen type IV (hCol IV), a major extracellular matrix (ECM) component of the human pancreatic islet, this platform supports more stable cellular maturation and sustained functional maintenance at a screening-compatible scale (Fig. 2). Given the critical role of ECM-mediated signaling in maintaining β-

cell identity and insulin secretory capacity, hCol IV supplementation provides a physiologically relevant microenvironment that closely reflects native human islet architecture [18, 23–25]. Furthermore, addition of hCol IV extended the functional maintenance period of islet organoids cultured in 96-well format, enabling long-term culture and prolonged drug testing. Consequently, this optimized system broadens its applicability to drug testing, including hormone stimulation assays and assessments of diverse stressors, such as inflammation.

In the present study, we established a T2D disease model using 96-well–based pancreatic islet organoid platform. Inflammatory factors, glucotoxicity, and lipotoxicity were applied to the islet organoids, and gene expression, GSIS and inflammatory cytokine secretion were subsequently evaluated, revealing characteristic features of T2D-associated β-cell impairment (Figs. 3 and 4). Traditionally, chemically induced animal models using sub-diabetogenic doses of streptozotocin (STZ) have been widely used to study T2D. However, these STZ-based models have limited ability to represent human-specific pancreatic β-cell dysfunction, due to species-specific differences and the insulin-resistant nature of T2D [26, 27]. In particular, substantial β-cell loss caused by STZ treatment leads to a disease state dominated by insulin deficiency, rather than the metabolic dysfunction–driven progression observed in human T2D. As a result, STZ-induced models may overestimate β-cell loss while underrepresenting functional impairment of surviving β-cells [26]. In contrast, our human pancreatic islet organoid–based T2D model captures both partial β-cell loss and functional impairment of surviving β-cells under diabetes-related metabolic stress, thereby more closely reflecting the pathophysiological features of human T2D. Although there were a moderate decrease in β-cell composition during T2D induction (Fig. 4C-E), basal insulin secretion under low-glucose conditions was preserved, whereas GSIS was markedly attenuated (Fig. 4A), indicating functional impairment of surviving β-cells. Consistent with this observation, immunofluorescence analysis confirmed the presence of insulin-positive cells following 3-day T2D induction (Fig. 4B), supporting the conclusion that impaired glucose responsiveness arises primarily from functional alterations in surviving β-cells rather than complete β-cell loss. Upon T2D induction, human pancreatic islet organoids exhibited a marked reduction in β-cell maturity markers, including MafB and PDX1, accompanied by decreased insulin gene expression. In contrast, stress- and dedifferentiation-associated genes such as IAPP and NGN3 were significantly upregulated, indicating loss of β-cell identity and activation of maladaptive transcriptional programs rather than acute β-cell death. Interestingly, α-cell proportion also decreased following T2D induction, which may reflect heightened islet-wide metabolic stress. Although β-cell dedifferentiation is often associated with trans-differentiation toward an α-cell lineage in advanced T2D [28], such lineage conversion was not observed under the current induction conditions. Nevertheless, increased NGN3 expression together with reduced expression of mature β-cell markers suggests that islet organoids entered a dedifferentiated state following T2D induction (Fig. 3).

Moreover, this model enables the evaluation of metabolic pathways associated with islet inflammation, which are difficult to evaluate using conventional chemically induced animal models. Targeting islet inflammation has been suggested by previous studies as a potential therapeutic strategy for slowing the progression of T2D [29]. Therefore, experimental models that accurately recapitulate islet inflammatory

responses are essential for drug development and therapeutic evaluation. In the pancreatic islet model, most inflammatory cytokines were upregulated following T2D induction, with CXCL1 and IL-8 being particularly amenable to simultaneous assessment at the secreted protein level by ELISA alongside the GSIS assay. By capturing inflammation-associated β-cell dysfunction in a controlled and reversible manner, this model overcomes key limitations of conventional animal models and offers a valuable tool for translational drug discovery.

Pharmacological treatment with GLP-1 receptor agonists and DPP-4 inhibitors further demonstrates that β-cell dysfunction in this model is reversible and could drug-responsive (Fig. 5). As expected, selected GLP-1 receptor agonists and DPP-4 inhibitors improved insulin secretion capacity in the islet organoid. In particular, tirzepatide, a novel dual agonist of the GIP and GLP-1 receptors, markedly enhanced insulin secretion in T2D-induced islet organoids. In contrast, no improvement was observed in RIN-m5 cells, an insulin-producing cell line derived from rat pancreatic islets (Figure S3B). This difference is potentially due to species-specific differences in GIP receptor responsiveness. The limited insulin-secretory effect of tirzepatide observed in rodent-derived RIN-m5 cells is consistent with previous reports demonstrating reduced GIP receptor responsiveness in rodent β-cells, highlighting species-specific differences in incretin signaling [30, 31]. A similar species-dependent pattern was also observed for GSK-1292263, which enhanced glucose-stimulated insulin secretion in rat insulinoma cells but not in human islet organoids (Figure S3). These findings underscore the importance of human-based islet models for assessing pharmacological responses during preclinical evaluation of T2D therapeutics.

In summary, we developed a human pancreatic islet organoid platform optimized for a screening-compatible scale that robustly recapitulates key features of T2D-associated β-cell dysfunction. By incorporating hCol IV within an ULA 96-well culture format, this system supports enhanced cellular maturation, prolonged functional maintenance, and stable assessment of glucose-responsive insulin secretion under disease-relevant stress conditions. The platform faithfully reproduces hallmark pathological characteristics of T2D, including β-cell dysfunction with moderate loss, dedifferentiation/inflammation-associated molecular changes, and impaired insulin secretion, while enabling human-specific evaluation of incretin-based therapeutics. Despite these advantages, however, several limitations should be acknowledged. The T2D induction protocol is based on a short-term induction strategy and may not fully capture the chronic and progressive nature of β-cell failure observed in patients. Nevertheless, this design enables the preservation of substantial β-cell mass while inducing functional dysfunction, thereby allowing the evaluation of reversible β-cell responses. In addition, although the organoid system recapitulates major endocrine cell populations, it lacks key components of the native islet microenvironment, including vascular, immune, and neuronal interactions. Future studies incorporating long-term disease induction, multi-organ microphysiological systems (MPS), as well as validation using patient-derived organoids and clinically advanced compounds, are expected to further enhance the physiological relevance and translational utility of this platform. Collectively, this organoid-based screening-compatible platform represents a physiologically relevant and scalable tool for drug screening and functional studies targeting β-cell dysfunction in T2D.

Declarations

Author Contributions

K.J.C.: Conceptualization, Data curation, Formal analysis, Investigation, Methodology, Validation, Visualization, Writing - original draft and review & editing. Y.N.: Data curation, Formal analysis, Investigation, Methodology, Validation, Visualization, Writing - original draft and review & editing. J.H.I: Data curation, Formal analysis, Investigation. H.M.Y.: Formal analysis, Investigation, Methodology, Writing - original draft. W.H.J.: Data curation, Formal analysis. S.B.P.: Writing - review and editing. B.K.: Writing - review and editing. M.S.: Writing - review and editing. K.Y.K.: Supervision, Writing– review and editing, Funding acquisition, Resources.

Funding

This study was supported by the Ministry of Trade, Industry & Energy (20017914 and 20009774) and the Korea Research Institute of Chemical Technology (KK2633-30) of Republic of Korea.

Data availability

The data used and/or analyzed during the current study are available from the corresponding author on reasonable request.

Ethics approval and consent to participate

Human embryonic stem cells (H1 hESCs) used in this study were obtained from WiCell Research Institute (Madison, WI, USA). The H1 cell line was originally derived from human blastocysts as previously described [32]. According to the provider, the cell line was derived with informed consent from donors and with approval from the appropriate institutional review boards (IRBs). The use of commercially available, de-identified cell lines did not require additional ethical approval.

Acknowledgements

The authors declare that they have not used AI-generated work in this manuscript.

Consent for publication

All authors agree to the publication of this work.

Competing interests

The authors declare no competing interests.

References

1. Brereton, M.F., M. Rohm, and F.M. Ashcroft, *beta-Cell dysfunction in diabetes: a crisis of identity?* Diabetes Obes Metab, 2016. **18 Suppl 1**(Suppl 1): p. 102-9.
2. Donath, M.Y. and S.E. Shoelson, *Type 2 diabetes as an inflammatory disease.* Nat Rev Immunol, 2011. **11**(2): p. 98-107.
3. Defronzo, R.A., *Banting Lecture. From the triumvirate to the ominous octet: a new paradigm for the treatment of type 2 diabetes mellitus.* Diabetes, 2009. **58**(4): p. 773-95.
4. Diane, A., L.I. Mohammed, and H.H. Al-Siddiqi, *Islets in the body are never flat: transitioning from two-dimensional (2D) monolayer culture to three-dimensional (3D) spheroid for better efficiency in the generation of functional hPSC-derived pancreatic beta cells in vitro.* Cell Commun Signal, 2023. **21**(1): p. 151.
5. Marshall, L.J., et al., *Poor Translatability of Biomedical Research Using Animals - A Narrative Review.* Altern Lab Anim, 2023. **51**(2): p. 102-135.
6. Du, Y., et al., *Human pluripotent stem-cell-derived islets ameliorate diabetes in non-human primates.* Nat Med, 2022. **28**(2): p. 272-282.
7. Tao, T., et al., *Engineering human islet organoids from iPSCs using an organ-on-chip platform.* Lab Chip, 2019. **19**(6): p. 948-958.
8. Eguchi, N., et al., *The Role of Oxidative Stress in Pancreatic beta Cell Dysfunction in Diabetes.* Int J Mol Sci, 2021. **22**(4).
9. Dinic, S., et al., *Oxidative stress-mediated beta cell death and dysfunction as a target for diabetes management.* Front Endocrinol (Lausanne), 2022. **13**: p. 1006376.
10. Dludla, P.V., et al., *Pancreatic beta-cell dysfunction in type 2 diabetes: Implications of inflammation and oxidative stress.* World J Diabetes, 2023. **14**(3): p. 130-146.
11. DeFronzo, R.A., et al., *Type 2 diabetes mellitus.* Nat Rev Dis Primers, 2015. **1**: p. 15019.
12. Witt, G., et al., *An automated and high-throughput-screening compatible pluripotent stem cell-based test platform for developmental and reproductive toxicity assessment of small molecule compounds.* Cell Biol Toxicol, 2021. **37**(2): p. 229-243.
13. French, A., et al., *Enabling consistency in pluripotent stem cell-derived products for research and development and clinical applications through material standards.* Stem Cells Transl Med, 2015. **4**(3): p. 217-23.
14. Hogrebe, N.J., et al., *Generation of insulin-producing pancreatic beta cells from multiple human stem cell lines.* Nat Protoc, 2021. **16**(9): p. 4109-4143.
15. Choi, S.J., et al., *Preparation of compact agarose cell blocks from the residues of liquid-based cytology samples.* Korean J Pathol, 2014. **48**(5): p. 351-60.
16. Llacua, L.A., M.M. Faas, and P. de Vos, *Extracellular matrix molecules and their potential contribution to the function of transplanted pancreatic islets.* Diabetologia, 2018. **61**(6): p. 1261-1272.
17. Zhu, Y., et al., *The collagen matrix regulates the survival and function of pancreatic islets.* Endocrine, 2024. **83**(3): p. 537-547.

18. Llacua, A., et al., *Extracellular matrix components supporting human islet function in alginate-based immunoprotective microcapsules for treatment of diabetes.* J Biomed Mater Res A, 2016. **104**(7): p. 1788-96.
19. Park, I.R., Y.G. Chung, and K.C. Won, *Overcoming beta-Cell Dysfunction in Type 2 Diabetes Mellitus: CD36 Inhibition and Antioxidant System.* Diabetes Metab J, 2025. **49**(1): p. 1-12.
20. Lv, C., et al., *beta-cell dynamics in type 2 diabetes and in dietary and exercise interventions.* J Mol Cell Biol, 2022. **14**(7).
21. Honzawa, N. and K. Fujimoto, *The Plasticity of Pancreatic beta-Cells.* Metabolites, 2021. **11**(4).
22. Rohm, T.V., et al., *Inflammation in obesity, diabetes, and related disorders.* Immunity, 2022. **55**(1): p. 31-55.
23. Yap, W.T., et al., *Collagen IV-modified scaffolds improve islet survival and function and reduce time to euglycemia.* Tissue Eng Part A, 2013. **19**(21-22): p. 2361-72.
24. Zhu, D., et al., *Enhanced viability and functional maturity of iPSC-derived islet organoids by collagen-VI-enriched ECM scaffolds.* Cell Stem Cell, 2025. **32**(4): p. 547-563 e7.
25. Brissova, M., et al., *Assessment of human pancreatic islet architecture and composition by laser scanning confocal microscopy.* J Histochem Cytochem, 2005. **53**(9): p. 1087-97.
26. Singh, R., M. Gholipourmalekabadi, and S.H. Shafikhani, *Animal models for type 1 and type 2 diabetes: advantages and limitations.* Front Endocrinol (Lausanne), 2024. **15**: p. 1359685.
27. Cefalu, W.T., *Animal models of type 2 diabetes: clinical presentation and pathophysiological relevance to the human condition.* ILAR J, 2006. **47**(3): p. 186-98.
28. Talchai, C., et al., *Pancreatic beta cell dedifferentiation as a mechanism of diabetic beta cell failure.* Cell, 2012. **150**(6): p. 1223-34.
29. Eguchi, K. and R. Nagai, *Islet inflammation in type 2 diabetes and physiology.* J Clin Invest, 2017. **127**(1): p. 14-23.
30. El, K., et al., *The incretin co-agonist tirzepatide requires GIPR for hormone secretion from human islets.* Nat Metab, 2023. **5**(6): p. 945-954.
31. Willard, F.S., et al., *Tirzepatide is an imbalanced and biased dual GIP and GLP-1 receptor agonist.* JCI Insight, 2020. **5**(17).
32. Thomson, J.A., et al., *Embryonic stem cell lines derived from human blastocysts.* Science, 1998. **282**(5391): p. 1145-7.

Table

Table 1. Primer sequence list for qPCR analysis

Gene	Forward	Reverse
IAPP	CAGCTGCAATGTTGGACAGAA	CGCAGCATGATGGCAGTTTAT
Insulin	CTACCTAGTGTGCGGGGAAC	ATTGTTCCACAATGCCACGC
CHGA	TGACCTCAACGATGCATTTC	CTGTCCTGGCTCTTCTGCTC
NKX6.1	GGCCTGTACCCCTCATCAAG	GAATAGGCCAAACGAGCCCT
NeuroD1	CCTTCGTTCAGACGCTTTGC	AGGCGACTGGTAGGAGTAGG
Glucagon	ATTTCCCAGAAGAGGTCGCC	CCCTGGCGGCAAGATTATCA
PDX1	GGGAAAACCCGCTCTCTCAG	CCAAGGTGGAGTGCTGTAGG
MafB	CATAGAGAACGTGGCAGCAA	ATGCCCGGAACTTTTTCTTT
Ngn3	CGGTAGAAAGGATGACGCCT	GGTCACTTCGTCTTCCGAGG
TXNIP	GGCCTTAAAGGATGCGGACT	CTTACGCCAGGAGGCCATTT
sXBP1	GCTGAGTCCGCAGCAGGT	CTGGGTCCAAGTTGTCCAGAAT
CHOP	AATGAACGGCTCAAGCAGGA	AGCCACTTCTGGGAAAGGTG
Atf3	ACCGTTAGGATTCAGGCAGC	TCACTCCACATCCCCTACGA
TRIB3	CCAACCCGATCCCATCTCTG	GCTGAGCGTGTAGTAGGGTG
MCP1	AGCAGCAAGTGTCCCAAAGA	TTGGGTTTGCTTGTCCAGGT
IL-1β	TCTTCCTGGGAGGGACCAAA	AGCCCTAGGGATTGAGTCCA
TNFa	CACAGTGAAGTGCTGGCAAC	AGGAAGGCCTAAGGTCCACT
iNOS	CGCATGACCTTGGTGTTTGG	CATAGACCTTGGGCTTGCCA
18S rRNA	GTAACCCGTTGAACCCCATT	CCATCCAATCGGTAGTAGCG

Figures

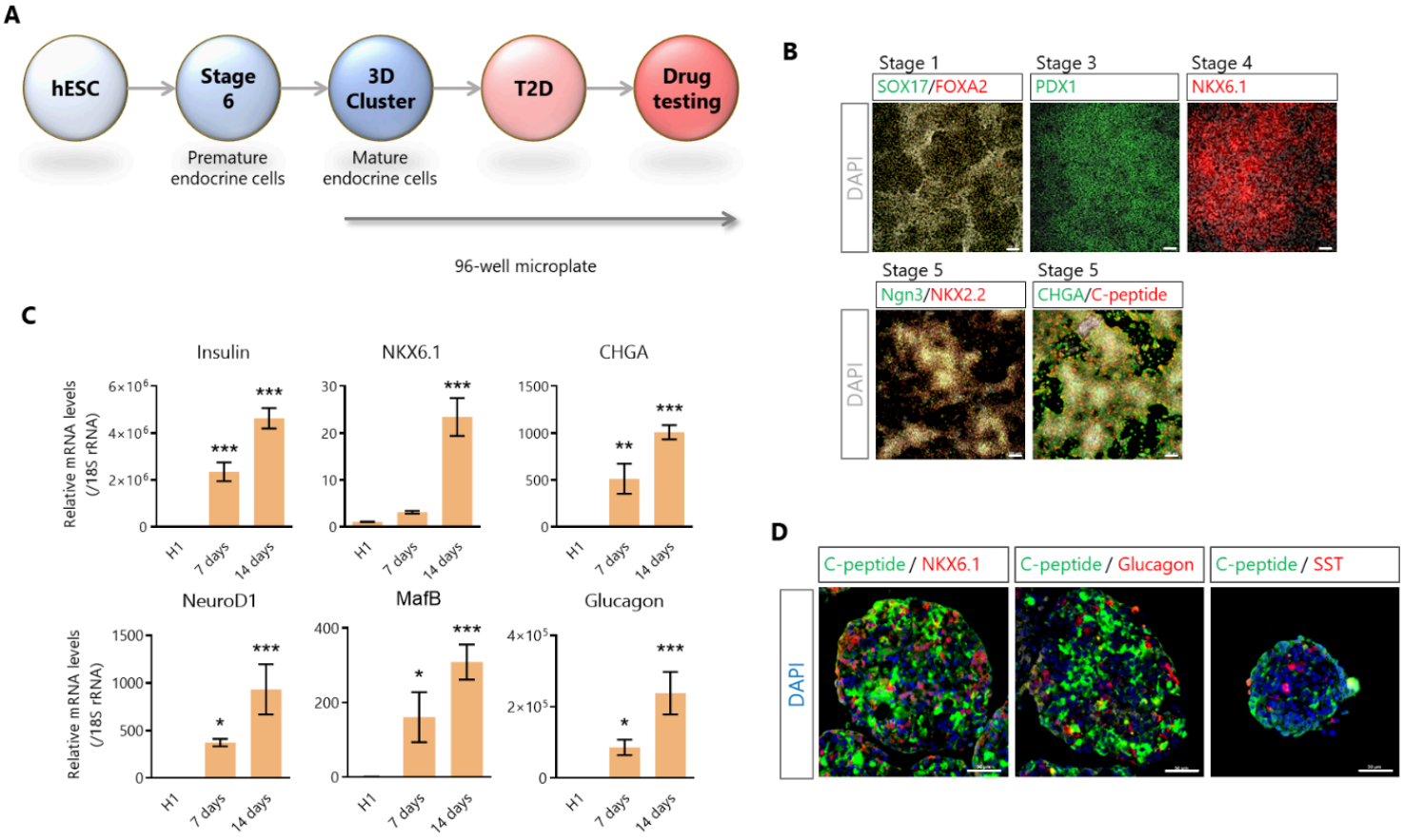


Figure 1

hESC-derived pancreatic β-cell generation. (A) The overall process of hESC-derived pancreatic islet organoid generation and T2D drug screening model. (B) Cell differentiation was confirmed from every stage via immunofluorescence staining assay with stage-specific expression marker. Nuclei were counterstained with DAPI (gray). Scale bar, 100 μm. (C) Mature β- and α-cell-related gene expression was analyzed by qPCR and presented as relative mRNA level vs. H1. Data is presented as a means ± S.D. (n = 3). The 18S rRNA was used for normalization. * $P < 0.05$, ** $P < 0.01$, *** $P < 0.001$ vs. H1 hESC (non-differentiated cell). (D) Immunofluorescence assay was performed after 3D cluster generation to assess the distribution of endocrine cells within organoid. Endocrine cells were stained with specific markers, and nuclei were counterstained with DAPI (blue). Scale bar, 50 μm.

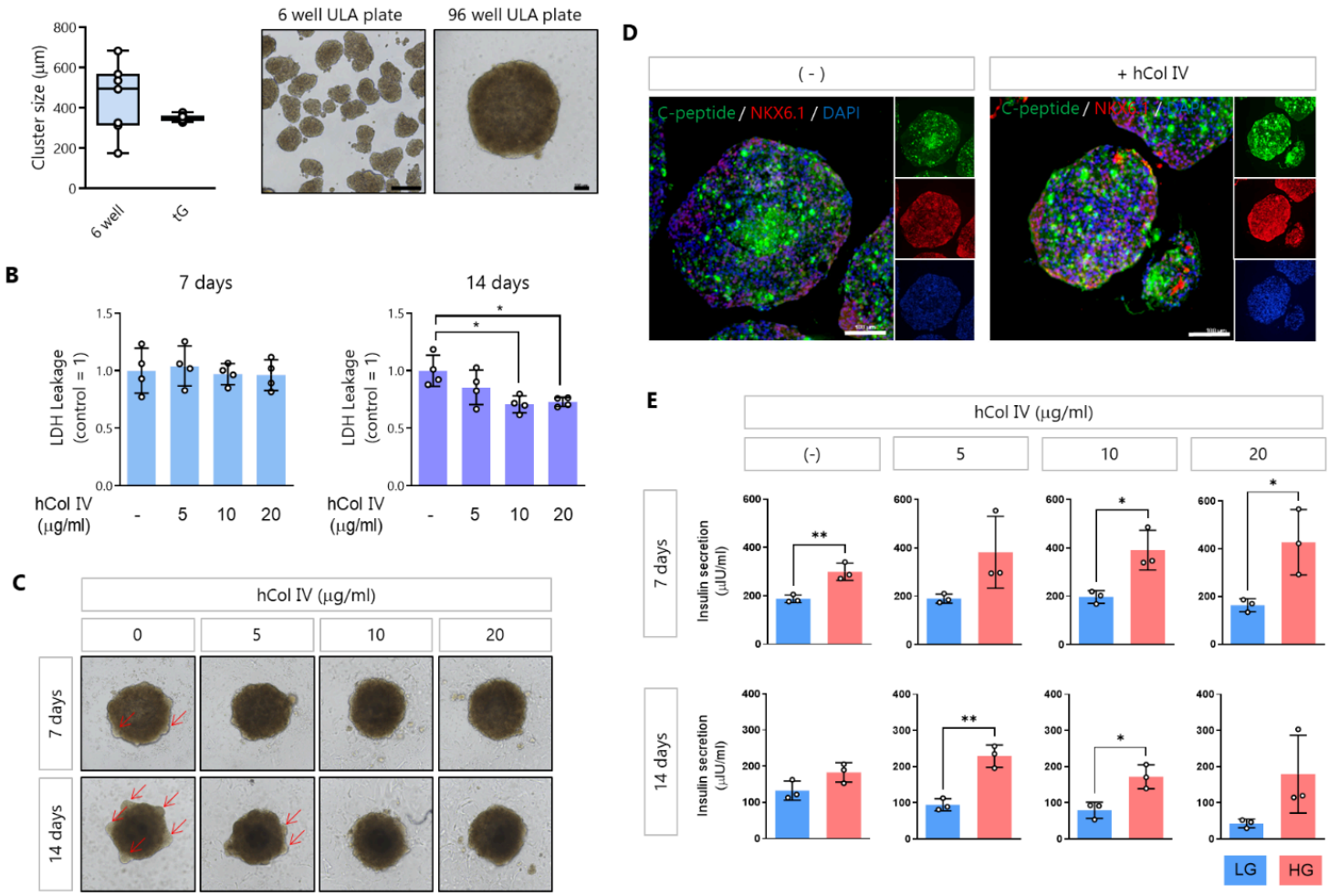


Figure 2

Pancreatic islet organoid generation for drug screening model. (A) Pancreatic islet organoids were generated on 6-well or 96-well ULA plate. After 2 days, cluster size (diameter, μm) were measured at a fixed magnification. The left panel shows the quantitative analysis of organoid diameter (n = 7), and the right panel shows representative bright-field images of the organoids. Scale bar, 200, 100 μm (B) Cytotoxicity of 3D β-cell organoids cultured with increasing concentrations of human collagen IV (hCol IV) was assessed by LDH release assay at 7 and 14 days of culture. Data are presented as fold change relative to the untreated control (control = 1). (C) Representative bright-field images of β-cell organoids cultured with different concentrations of hCol IV (0, 5, 10, and 20 μg/mL) for 7 and 14 days. Red arrows indicate non-specified or irregular spheroid morphology observed under ECM-free and ECM low conditions. (D) Immunofluorescence staining of 3D β-cell organoids cultured in the absence or presence of hCol IV, showing enhanced expression and spatial organization of C-peptide (green) and NKX6.1 (red) under hCol IV conditions. Nuclei were counterstained with DAPI (blue). Scale bar, 100 μm. (E) Glucose-stimulated insulin secretion (GSIS) assay of β-cell organoids cultured with increasing concentrations of hCol IV for 7 and 14 days. Insulin secretion under low glucose (LG) and high glucose (HG) conditions is shown. Data are presented as mean ± S.D, (n = 3). $^{*}P < 0.05$, $^{**}P < 0.01$ compared with LG conditions.

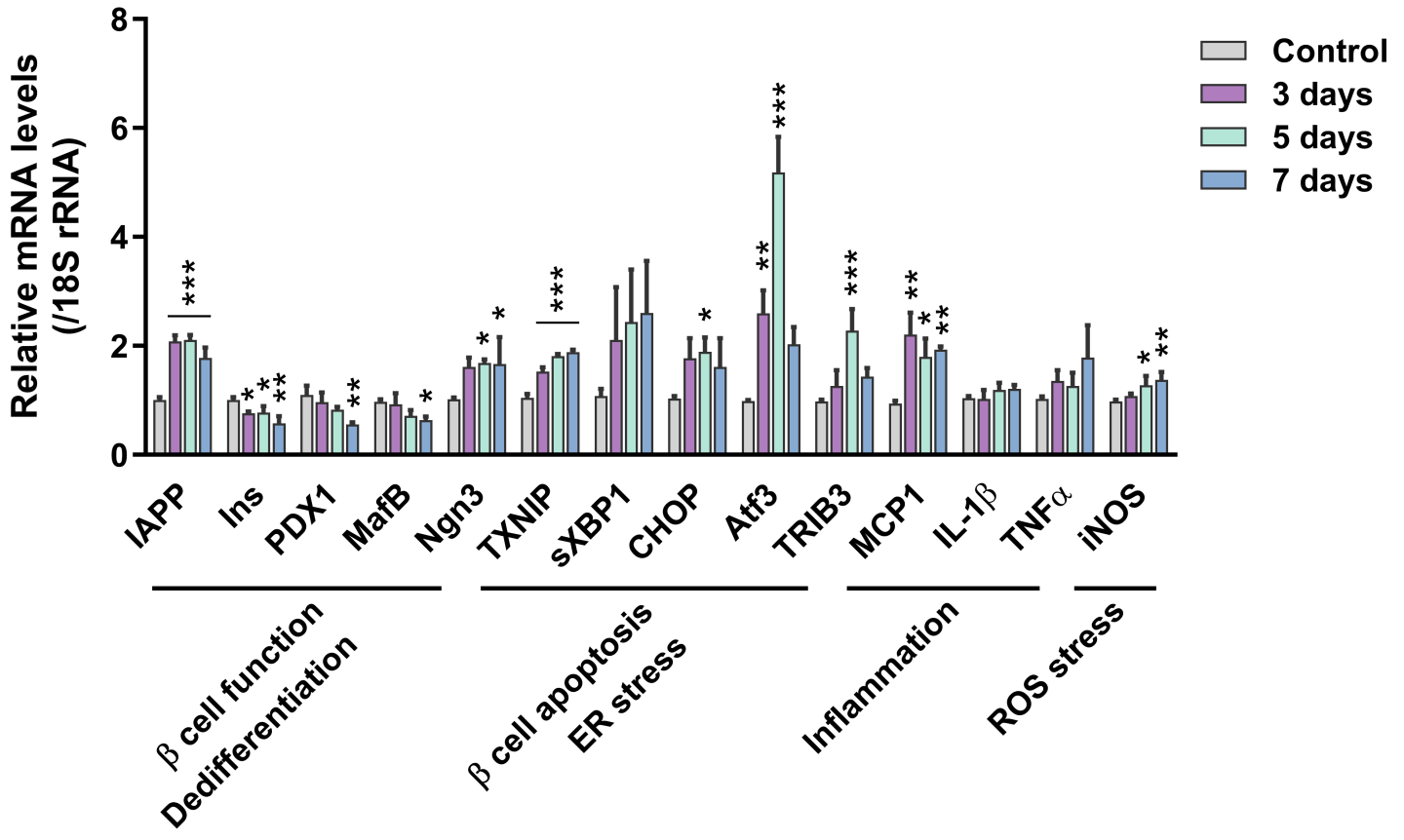


Figure 3

Induction of Type 2 diabetes–like molecular signatures in hESC-derived β-cell organoids. β-cell organoids were exposed to Type 2 diabetes–mimicking conditions, and the expression of genes associated with β-cell identity, stress responses, and inflammation was analyzed by quantitative PCR (qPCR) at the indicated time points (3, 5, and 7 days). Relative mRNA expression levels of β-cell function and de-differentiation markers (IAPP, Ins, PDX1, MafB, and Ngn3), ER stress and apoptosis-related markers (TXNIP, sXBP1, CHOP, Atf3, and TRIB3), inflammatory markers (MCP1, IL-1β, and TNF-α), and oxidative stress marker (iNOS) are shown. Expression levels were normalized to 18S rRNA and presented as fold change relative to the normal condition. Data are shown as mean ± S.D. (n = 3). $^{*}P < 0.05$, $^{**}P < 0.01$, $^{***}P < 0.001$ compared with normal cell.

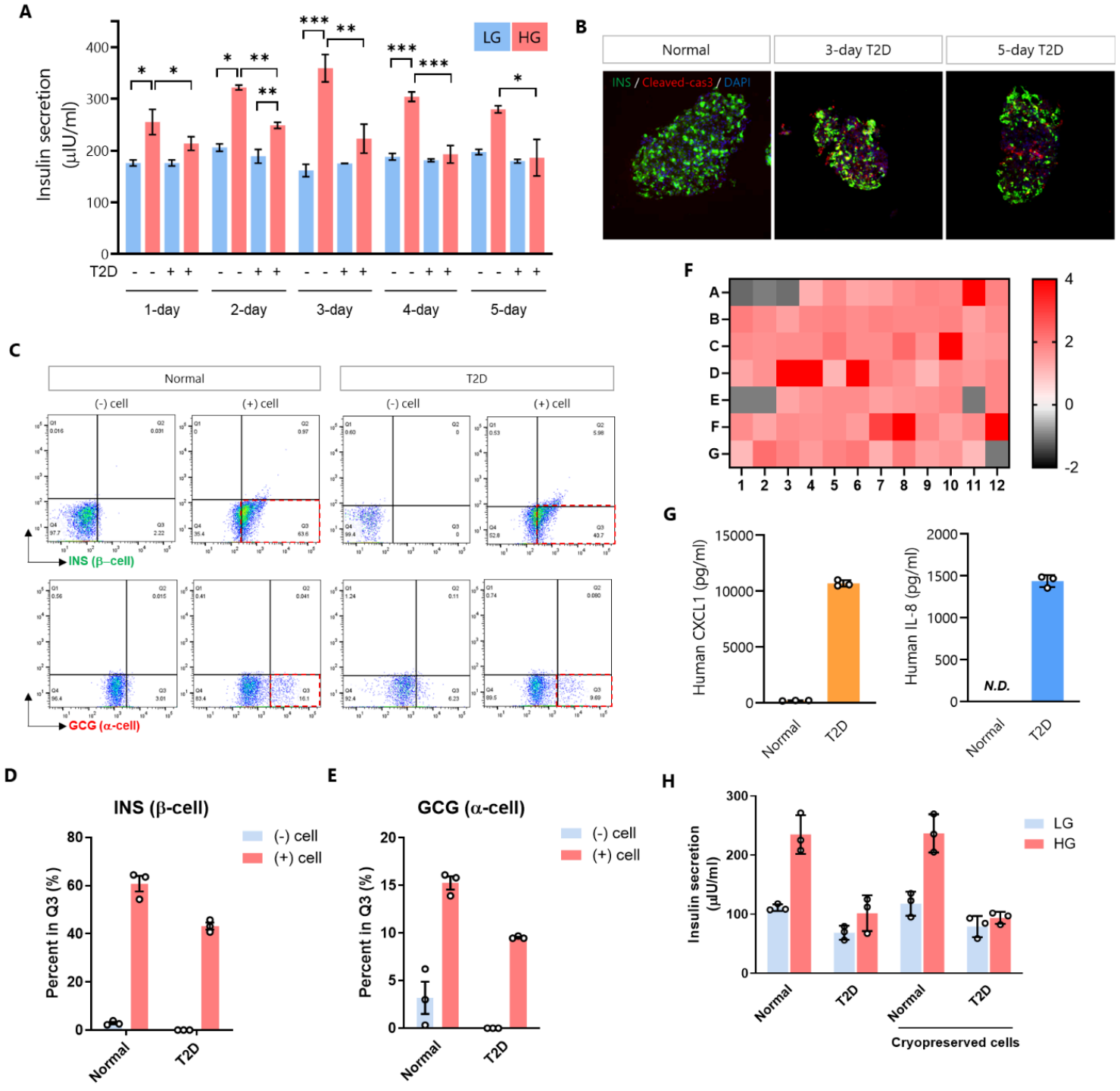


Figure 4

Time-dependent impairment of β-cell function and increased apoptosis following T2D induction in hESC-derived pancreatic β-cell organoids. (A) Static glucose-stimulated insulin secretion (GSIS) analysis of pancreatic β-cell organoids following T2D induction for 1 to 5 days. Insulin secretion under low-glucose (LG) and high-glucose (HG) conditions was quantified at each time point. Pancreatic organoids were induced T2D for indicated date, and static GSIS analysis was conducted. (B) Representative immunofluorescence images of pancreatic β-cell organoids under normal conditions or after 3-day and 5-day T2D induction, stained for insulin (INS, green), cleaved caspase-3 (red), and DAPI

(blue). Scale bars, XX μm. (C) Flow cytometric analysis of cell composition in pancreatic islet organoids. Representative flow cytometry dot plats showing insulin (INS) and glucagon (GCG) expression in normal and T2D-induced organoids. Quantification of INS+ β-cells (D) and GCG+ α-cells (E) gated in the Q3 quadrant is presented as a bar graph. (F) Inflammatory cytokines gene expression was analyzed by qPCR array and visualized as a heatmap. Total 84 inflammatory cytokine-related genes were quantitatively assessed and are presented as fold-regulation relative to normal pancreatic organoids (n = 3). Color intensity reflects normalized expression levels relative to the normal condition. (G) The secreted protein levels of CXCL1 and IL-8 were measured using ELISA. Following 3 days of T2D induction, cell culture supernatants were collected and cytokine levels were analyzed. N.D., not detected. (H) GSIS was compared between β-cell organoids generated by continuous differentiation and those derived from cells cryopreserved at an intermediate differentiation stage and subsequently matured. GSIS was assessed under LG and HG conditions in both normal and T2D-induced organoids. Insulin secretion is presented as μU/mL. Data are presented as mean ± S.D. (n = 3). $^{*}P < 0.05$, $^{**}P < 0.01$, $^{***}P < 0.001$.

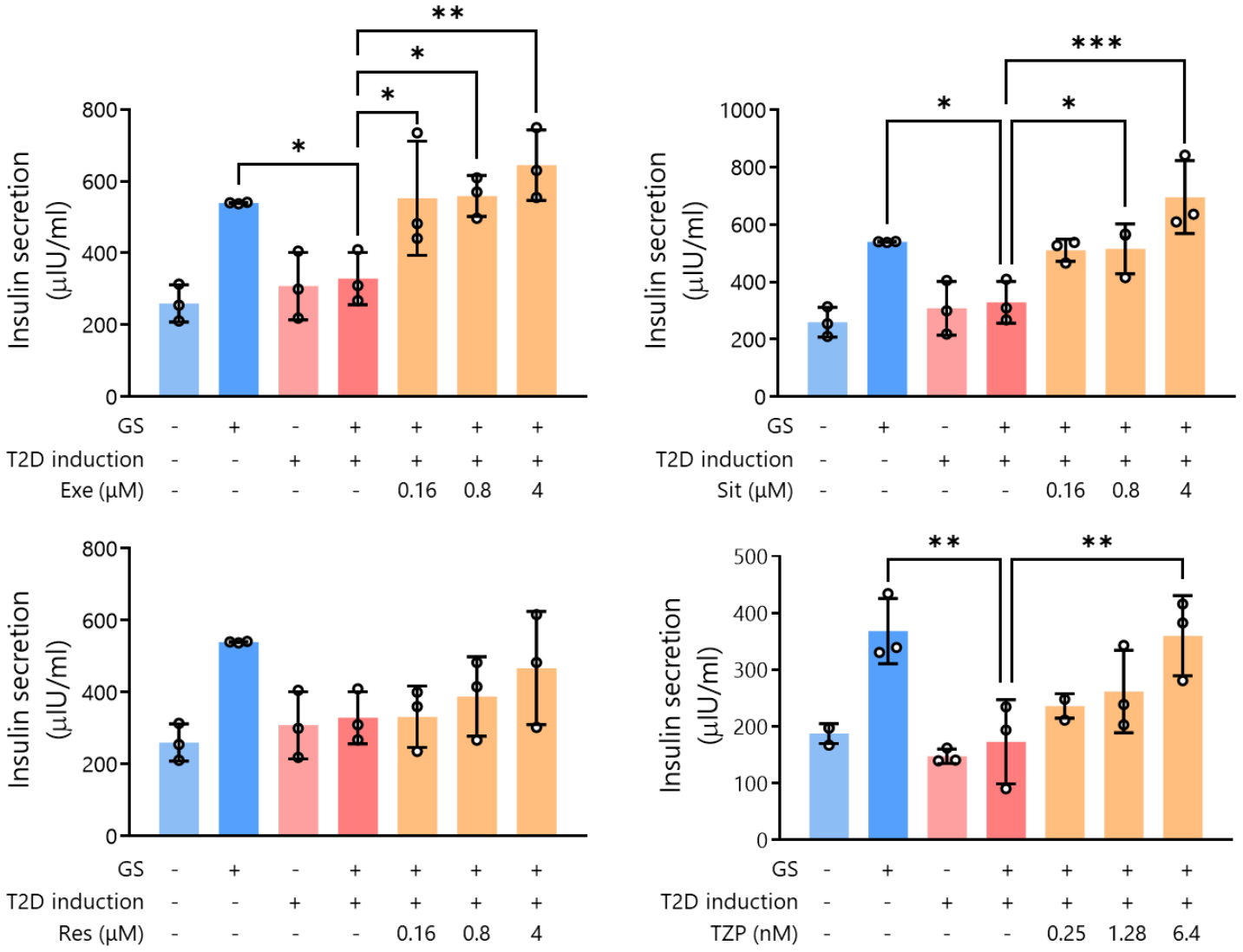


Figure 5

Evaluation of reference antidiabetic drugs using GSIS assay in T2D-induced β-cell organoids. Glucose-stimulated insulin secretion (GSIS) assay was performed to assess the functional responsiveness of T2D-induced β-cell organoids following treatment with reference antidiabetic drugs. Organoids were exposed to T2D-inducing conditions and subsequently treated with Exendin-4 (Exe, μM), Sitagliptin (Sit, μM), Resveratrol (Res, μM), or Tirzepatide (TZP, nM) for 2 days at the indicated concentrations. Insulin secretion was measured under low glucose (GS−) or high glucose (GS+) conditions. Data are presented as insulin concentration (μU/mL) and shown as mean ± S.D. (n = 3). Statistical significance is indicated as $^{*}P < 0.05$, $^{**}P < 0.01$, $^{***}P < 0.001$.

Supplementary Files

This is a list of supplementary files associated with this preprint. Click to download.

- 4.Additionalfile.docx